Available online at www.sciencedirect.com
SCIENCE DIRECT®
Biochemical and Biophysical Research Communications 322 (2004) 1–8
BBRC
www.elsevier.com/locate/ybbrc

Mouse spermine oxidase: a model of the catalytic cycle and its inhibition by N,N^1-bis(2,3-butadienyl)-1,4-butanediamine ☆

Andrea Bellelli [a,*], Stefano Cavallo [a], Laura Nicolini [b], Manuela Cervelli [c], Marzia Bianchi [c], Paolo Mariottini [c], Massimo Zelli [c], Rodolfo Federico [c]

[a] *Dipartimento di Scienze Biochimiche "Alessandro Rossi Fanelli," Università di Roma "La Sapienza" and Istituto di Biologia e Patologia Molecolari del CNR, I-00185 Rome, Italy*
[b] *Servizio Biologico, Istituto Superiore di Sanità, I-00161 Rome, Italy*
[c] *Dipartimento di Biologia, Università "Roma Tre," I-00146 Rome, Italy*

Received 23 June 2004
Available online 29 July 2004

Abstract

Spermine oxidase (SMO) is a recently described flavoenzyme belonging to the class of polyamine oxidases (PAOs) and participating in the polyamine metabolism in animal cells. In this paper we describe the expression, purification, and characterization of the catalytic properties of a recombinant mouse SMO (mSMO). The purified enzyme has absorbance peaks at 457 nm ($\varepsilon = 11\,mM^{-1}\,cm^{-1}$) and 378 nm, shows a molecular mass of ~63 kDa, and has K_m and k_{cat} values of 170 μM and $4.8\,s^{-1}$, using spermine as substrate; it is unable to oxidize other free or acetylated polyamines. The mechanism-based PAO inhibitor N,N^1-bis(2,3-butadienyl)-1,4-butanediamine (MDL72,527) acts as a competitive inhibitor of mSMO, with an apparent dissociation constant $K_i = 63\,\mu M$. If incubated for longer times, MDL72,527 yields irreversible inhibition of the enzyme with a half-life of 15 min at 100 μM MDL72,527. The mMSO catalytic mechanism, investigated by stopped flow, is consistent with a simple four-step kinetic scheme.

Keywords: Polyamine oxidase; Spermine oxidase; Mouse; Protein engineering; Stopped flow

Animal polyamine oxidases (PAOs, EC 1.5.3.11) are flavin adenine dinucleotide (FAD) containing enzymes involved in the inter-conversion metabolism of polyamines, oxidizing N^1-acetylderivatives of spermine (Spm) and spermidine (Spd) into Spd and putrescine (Put), respectively, and 3-acetamidopropanal and H_2O_2 [1–3]. Since this enzyme plays a crucial role in polyamine catabolism, the mammalian PAO has been considered an important drug target and, in fact, it has been shown that a number of polyamine analogues have an antitumor effect in different cell lines [4–7]. In particular, PAO has been found in all vertebrate tissues [2] and has been purified by chromatographic methods and shown to be subcellularly localized in both cytoplasm and peroxisomes [8–10]. Recently, Vujcic et al. [11] applied a functional genomics approach to identify murine and human PAOs, and demonstrated that PAO expression is inducible by polyamine analogues.

Wang et al. [12,14], Vujcic et al. [13], and Cervelli et al. [15] have reported the cloning and characterization of a novel mammalian PAO capable of oxidizing preferentially Spm and for this reason named spermine oxidase (SMO). In particular, this enzyme was expressed in an in vitro transcription/translation system [12], into transiently transfected human kidney 293 cells [13] and

☆ *Abbreviations:* FAD, flavin adenine dinucleotide; PAO, polyamine oxidase; mSMO, mouse spermine oxidase; Pi, phosphate buffer.

* Corresponding author. Fax: +39064440062.
E-mail address: andrea.bellelli@uniroma1.it (A. Bellelli).

0006-291X/$ - see front matter © 2004 Elsevier Inc. All rights reserved.
doi:10.1016/j.bbrc.2004.07.074

into *Escherichia coli* BL21 DE3 cells [14,15]. On the basis of these studies, it was postulated that in addition to the traditional inter-conversion pathway in which Spm is first acetylated by spermidine/spermine N^1-acetyltransferase and then oxidized by PAO, mammalian cells contain an enzyme capable of directly oxidizing Spm to Spd. The single copy murine *SMO* gene (*mSMO*) codes for at least nine splicing variants and, as predicted from the amino acid sequences, only two of them have been proved to be active [16]. These two isoforms, described as mSMOα (the major form) and mSMOμ (possessing a thirty amino acid extra domain), show identical biochemical properties but different subcellular localization [16]. In the present work we refer to the major form mSMOα, herein simply named as mSMO. To enhance knowledge of mSMO, the recombinant mature form has been expressed in *E. coli* BL21 DE3 cells, purified by three chromatographic steps, and characterized. We carried out inhibition assay experiments on the mSMO enzymatic activity in the presence of the PAO inhibitor N,N^1-bis(2,3-butadienyl)-1,4-butanediamine (MDL72,527).

Furthermore, this paper describes the biochemical features of the mSMO mature form, and its catalytic mechanism, as investigated by steady state and rapid kinetic techniques. The experimental data proved consistent with a minimal kinetic scheme involving four enzyme intermediates, two oxidized and two reduced (i.e., colorless).

Experimental

Chemicals. Spd, Spm, N^1-acetylspermidine (N^1-AcSpd), N^1-acetylspermine (N^1-AcSpm), and Put were purchased from Sigma. MDL72,527 was a generous gift from Dr. M. De Agazio (Consiglio Nazionale delle Ricerche, Area della Ricerca di Roma—Montelibretti).

DNA methodology and construction of mSMO expression plasmid. The methods described by Sambrook et al. [17] were used for the extraction and manipulation of plasmid DNA and general DNA in vitro methods. Nucleotide sequencing was obtained for both strands using the automated fluorescent dye terminator technique (Perkin–Elmer ABI model 373A). In order to clone the murine cDNA (Image Clone 2647695, GenBank Accession No. BC004831) by PCR amplification, the full-length cDNA was generated possessing modified 5′ and 3′ ends. In particular, the two following synthetic oligonucleotides were used to introduce *Nde*I and *Xho*I restriction sites at the 5′ and 3′ ends of mSMO cDNA: SMO1-DIR, 5′-TTTCATATGCAAAGTTGTGAATCCAG-3′ and SMO2-REV, 5′-AAATATCTCGAGGGAACACATTTGGCA GTGAGG-3′, respectively. The amplified PCR product was restricted by *Nde*I and *Xho*I and ligated with the restricted *Nde*I/*Xho*I pET17b vector (Novagen), to obtain the genetic construct containing the mature form of mSMO, named pET17b/mSMO. The recombinant cDNA construct was resequenced to check the accuracy of the nucleotide sequence and then utilized to transform *E. coli* BL21 DE3 (Novagen) competent cells.

Culture conditions and expression of mSMO in E. coli cells. Fermentations were performed on a medium containing bacto tryptone (1% w/v), yeast extract (0.5%, w/v), NaCl (1% w/v), ampicillin (50 μg/ml), and chloramphenicol (34 μg/ml). Propylene glycol monolaurate (0.006% v/v) was also added to the fermentor medium as an antifoaming agent and the pH was adjusted to 7.0 after autoclaving. For fermentor production, *E. coli* BL21 DE3 cells were transformed with pmSMO plasmid and then grown for 18 h with 120 rpm orbital shaking at 37 °C in a 2 L Erlenmeyer flask containing 1 L medium and added to the fermentor as a 2% (v/v) inoculum. Batch fermentations were carried out using a 70-L B-Braun Fermentor (mod.Biostat UD-50) with a working volume of 50 L. Aeration, temperature, and agitation were maintained at 1/1 vol medium per minute, at 37 °C and 200 rpm (impeller 125-mm diameter), respectively. The pH was controlled with an Ingold glass sterile electrode. When the optical density (OD, spectrophotometrically measured at 600 nm) reached the value of 0.700, the temperature of the medium was lowered at 28 °C and IPTG (0.4 mM) was added to the broth culture. The culture was stopped after 7 h of growth (OD value of 1.530). Cells were then centrifuged (Alpha-Laval Sharples mod.T1P) at 50.000 rpm and the biomass obtained (120-g) was stored at −80 °C.

Purification of mSMO. The *E. coli* BL21 DE3 cells were harvested by centrifugation at 4 °C for 10 min at 10,000*g*, washed with 0.4 culture volumes of 30 mM Tris–HCl, pH 8.0, 20% sucrose, and 1 mM EDTA, and incubated, for 5–10 min at room temperature. A 20-g amount of frozen bacterial pellet was added with 40 g of alumina Type A.5 (Sigma) in 5 volumes of 50 mM sodium phosphate (NaPi), pH 6.5, containing 1 mM PMSF and 5 mM DTT, and manually lysed in a mortar. The cell-alumina paste was centrifuged at 5000*g* for 30 min and the pellet was rehomogenized for 15 min in 2 volumes of the same buffer and centrifuged again at 5000*g*. The supernatants were combined and cleared by centrifugation at 30,000*g* for 30 min and loaded onto a Hi Trap Q Sepharose HP (D = 0.5 cm, V = 5 ml, flowrate = 4 ml/min). The column was washed with 20 volumes of 50 mM NaPi, pH 6.5 and bound proteins were eluted with a linear gradient of 0.1–0.4 M NaCl in 50 mM NaPi, pH 6.5. mSMO containing fractions (around 0.3 M NaCl) were combined, the pH was adjusted to 7.0 with 1 M NaOH, then added with $(NH_4)_2SO_4$ to a final concentration of 1 M, and finally loaded onto a Hi Trap butyl Sepharose FF (D = 1.6 cm, L = 05 cm, V = 10 ml, flowrate = 5 ml/min). The column was washed with the same buffer until the A_{280} of the eluate lowered below 0.05 and then eluted with a linear gradient of 1000–250 mM $(NH_4)_2SO_4$ in 0.3 M NaCl/50 mM NaPi, pH 7.0. Fractions with the highest mSMO activity [around 0.5 M $(NH_4)_2SO_4$] were pooled and concentrated in an ultrafiltration cell (Amicon, Danvers, MA, USA) equipped with an XM 30 filter. Finally, the enzyme was loaded onto a size-exclusion chromatography column on a Superdex 200 HR 10/30 (Pharmacia Biotech, Uppsala, Sweden) and eluted with 50 mM NaPi, pH 7.0, containing 0.3 M NaCl at a flow rate of 1 ml/min. Fractions with high enzymatic activity were pooled and concentrated by ultrafiltration as described above. All chromatographic steps were performed on a FPLC system from Pharmacia at room temperature and fractions were immediately chilled and stored at 2 °C.

Enzyme and cofactor spectra. FAD was released from a solution of the mSMO enzyme (400 μg) in 100 μl of 0.2 M potassium phosphate (KPi) buffer, pH 7.0, with 9-fold volume of methanol. The solution was boiled for 15 min, cooled on ice, and centrifuged at 14,000*g* for 15 min at 4 °C. The absorption spectra of the native mSMO (400 μg in 1 ml of 0.2 M KPi buffer, pH 7.0) and methanol cofactor solution were recorded in a Philips PU 8820 UV/VIS spectrophotometer.

Enzyme activity and inhibition assays. Enzyme activity was measured spectrophotometrically by following the formation of a pink adduct (ε_{515} = 26 $mM^{-1}cm^{-1}$) as a result of the oxidation and condensation of 4-aminoantipyrine (Sigma) with 3,5-dichloro-2-hydroxybenzenesulfonic acid (Sigma) catalyzed by horseradish peroxidase [18]. The measurements were performed in either 0.2 M NaPi buffer, pH 8.5, or 0.2 M glycine buffer, pH 9.5, or 0.083 M sodium borate buffer, pH 9.0. Enzyme activities were expressed in International Units (IU), whose definition is such that one unit converts 1 μmol of substrate min^{-1}. Protein content was estimated by the method of Bradford [19] with bovine albumin as a standard. SDS–PAGE was performed according to the method of Laemmli [20]. In the inhibition enzyme

assay, the mSMO concentration ranged between 20 and 50 nM and that of Spm ranged between 20 and 200 μM (i.e., [E] < [S] and [E] < [I], where [E], [S], and [I] indicate the enzyme, the substrate, and the inhibitor concentrations; moreover, $0.1 \times K_m < [I] < 10 \times K_I$, where K_I is the apparent dissociation equilibrium constant for the formation of the reversible enzyme:inhibitor complex). The assay time was 30 s; this is important because over longer incubation times the inhibition by MDL72,527 becomes irreversible. The K_I for inhibition by MDL72,527 was determined from the linear dependence of the K_m^{app}/K_m^0 ratio on the inhibitor concentration [I], according to Eq. (1):

$$K_m^{app}/K_m^0 = K_I^{-1} \cdot [\mathrm{MDL72,527}] + 1 \quad (1)$$

where K_m^{app} is the apparent Michaelis constant determined at a fixed inhibitor concentration and K_m^0 is the intrinsic Michaelis constant determined in the absence of the inhibitor. Values of K_m^0 and K_m^{app} (see Eq. (1)) for the Spm oxidation by mSMO were determined from the dependence of the initial velocity on the substrate concentration according to the Michaelis–Menten equation in the absence and presence of the inhibitor, respectively. As expected for a simple competitive inhibition system, values of V_{max} were unaffected by the inhibitor.

Incubation of the enzyme with MDL72,527 for several minutes results in irreversible inhibition; therefore, at least two enzyme-inhibitor complexes must be hypothesized, one reversible, the other irreversible. Although in principle the two may be unrelated to each other, a plausible sequential reaction scheme is presented in Scheme 1. In this scheme irreversible inhibition is an unlikely evolution of the reversible complex, and the relationship between the apparent and intrinsic rate constants of inhibition is as follows:

$$k_{app} = [I]k_{intr}/([I] + K_I) \quad (2)$$

Rapid kinetic experiments were carried out using an Applied Photophysics SX18 stopped flow apparatus (Applied Photophysics, Leatherhead, UK), equipped with a photodiode array detector capable of reading absorbance spectra over the UV–Vis range. Two types of experiments were devised: (i) the oxidized enzyme, dissolved in air equilibrated buffer, was mixed with different concentrations of Spm dissolved in air equilibrated buffer; oxygen concentration after mixing was 270 μM; (ii) the enzyme, dissolved in degassed buffer containing different concentrations of Spm, was mixed with air equilibrated buffer; oxygen concentration after mixing was 135 μM. In experiment (i) the enzyme is oxidized before mixing and the first kinetic process is reduction by Spm; by contrast in experiment (ii) the enzyme is reduced before mixing and the first kinetic process observed is oxidation by dioxygen. Single turnover experiments were carried out by rapidly mixing in the stopped flow apparatus the oxidized enzyme with Spm at the desired concentration. Both solutions were carefully degassed and equilibrated under 1 atm of pure N_2. Moreover, to avoid contamination by atmospheric oxygen, 5 mM glucose and trace amounts of glucose oxidase and catalase (both from Sigma, St. Louis, MO, USA) were added to both solutions.

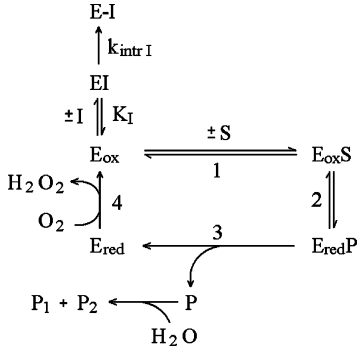

Scheme 1. Minimal kinetic scheme capable of accounting for the observed reactions. This scheme was used to fit a complex set of time courses collected at 460 nm; it also describes the two-step mechanism of inhibition by N,N^1-bis(2,3-butadienyl)-1,4-butanediamine (represented as I).

Data were globally analyzed by means of a least squares non-linear minimization routine capable of numerical integration of stiff differential equations developed using the Borland Pascal Compiler (version 7.0, Borland, Scotts Valley, CA, USA) [21]. Preliminary analyses were carried out using the commercially available package Matlab (version 5.0, The Math Works, Natick, MA, USA); these involve the detection of the minimal number of spectroscopically distinguishable intermediates.

Several kinetic mechanisms were explored, and the minimal catalytic scheme capable of a satisfactory fit of the experimental data is reported below (Scheme 1). The difference kinetic equations derived from Scheme 1 are as follows:

$$\delta[\mathrm{Eox}]/\delta t = [\mathrm{EoxS}]k_{-1} + [\mathrm{Er}][\mathrm{O_2}]k_4 - [\mathrm{Eox}][\mathrm{S}]k_{+1} \quad (3)$$

$$\delta[\mathrm{EoxS}]/\delta t = [\mathrm{Eox}][\mathrm{S}]k_{+1} + [\mathrm{ErP}]k_{-2} - [\mathrm{EoxS}](k_{-1} + k_{+2}) \quad (4)$$

$$\delta[\mathrm{ErP}]/\delta t = [\mathrm{EoxS}]k_{+2} - [\mathrm{ErP}](k_{-2} + k_3) \quad (5)$$

$$\delta[\mathrm{Er}]/\delta t = [\mathrm{ErP}]k_{+3} - [\mathrm{Er}][\mathrm{O_2}]k_4 \quad (6)$$

$$\delta[\mathrm{S}]/\delta t = -\delta[\mathrm{P}]/\delta t = [\mathrm{EoxS}]k_{-1} - [\mathrm{Eox}][\mathrm{S}]k_{+1} \quad (7)$$

$$\delta[\mathrm{O_2}]/\delta t = -\delta[\mathrm{H_2O_2}]/\delta t = [\mathrm{Er}][\mathrm{O_2}]k_4 \quad (8)$$

The kinetic model assigns the observed optical density changes to the conversion of the oxidized (Eox or EoxS) into the reduced enzyme (Er or ErP), thus it requires only two extinction coefficients at each wavelength submitted to analysis, one for the oxidized mSMO (shared by species Eox and EoxS), the other for the reduced derivatives (Er and ErP).

In an enzyme requiring two substrates (in the present case O_2 and Spm), the steady state experiments are usually carried out at fixed concentration of one substrate, by systematically varying the other; thus, the values of K_m and k_{cat} for the varied substrate depend on the concentration of the fixed substrate. In our opinion it is important that the kinetic rate constants determined by stopped flow are used to calculate the corresponding steady state parameters and that these are compared with the values measured directly, since this procedure provides a stringent test of the consistency of the model. This analysis was carried out according to standard procedures (e.g. [20]); briefly, Eqs. (3)–(6) were equated to zero (the steady state approximation), then the concentration of Er was taken as a reference and all other enzyme derivatives were expressed as a function of [Er] and the kinetic constants, to obtain the catalytic rate equation:

$$\begin{aligned} v = {} & [\mathrm{mSMO}][\mathrm{S}]k_{+1}k_{+2}k_3[\mathrm{O_2}]k_4/([\mathrm{S}]k_{+1}k_{+2}k_3 \\ & + k_{+1}k_{+2}[\mathrm{O_2}]k_4 + [\mathrm{S}]k_{+1}k_{-2}[\mathrm{O_2}]k_4 + [\mathrm{S}]k_{+1}k_3[\mathrm{O_2}]k_4 \\ & + k_{+2}k_3[\mathrm{O_2}]k_4 + k_{-1}k_{-2}[\mathrm{O_2}]k_4 + k_{-1}k_3[\mathrm{O_2}]k_4) \end{aligned} \quad (9)$$

By assuming either [S] = ∞ or [O_2] = ∞, we find the two k_{cat} values:

$$\begin{aligned} k_{cat\ S,[O_2]=constant} = {} & k_{+2}k_3k_4[\mathrm{O_2}]/(k_{+2}k_3 + k_{+2}k_4[\mathrm{O_2}] \\ & + k_{-2}k_4[\mathrm{O_2}] + k_3k_4[\mathrm{O_2}]) \end{aligned} \quad (10)$$

$$\begin{aligned} k_{cat\ O_2,[S]=constant} = {} & [\mathrm{S}]k_{+1}k_{+2}k_3/([\mathrm{S}]k_{+1}k_{+2} + [\mathrm{S}]k_{+1}k_{-2} \\ & + [\mathrm{S}]k_{+1}k_3 + k_{-1}k_{-2} + k_{-1}k_3 + k_{+2}k_3) \end{aligned} \quad (11)$$

The K_m values were derived by equating the catalytic rate Eq. (9) to 1/2 of the corresponding k_{cat} and solving for either O_2 or S. All the relevant kinetic parameters for mSMO are reported in Tables 2 and 3.

Results

Purification of E. coli expressed mSMO

High level expression of mSMO was obtained from pET17b/mSMO transformed *E. coli* BL21 DE3 cells after incubation with 1 mM IPTG as described under Experimental. Due to the relatively high level of mSMO protein in the starting material, we developed a highly efficient purification protocol. The frozen bacterial pellet was mechanically homogenized, then the homogenate was cleared by centrifugation and the supernatant was purified in three chromatographic steps to obtain a homogeneous product consisting of mSMO protein. The summary of the purification is presented in Table 1. Starting with 20-g of frozen bacterial pellet from 8 l culture broth a total of 12-mg homogeneous mSMO protein was purified. The final preparation had a specific activity of 5 U/mg, corresponding to a k_{cat} of 4.8 s^{-1}, the purification was 16.1-fold and the yield was about 21% of the total activity in the homogenate.

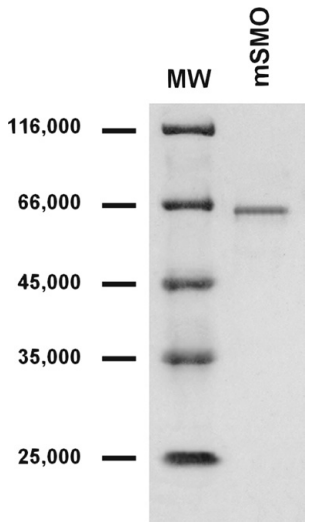

Fig. 1. Purified recombinant mSMO protein analysis. SDS–PAGE analysis of the recombinant mSMO (1 μg of the purified enzyme) after Coomassie brilliant blue staining. MW, protein molecular weight marker (MBI Fermentas).

Molecular properties and substrate specificity of mSMO

The purified mSMO protein is yellow colored with visible absorption maxima at 457 and 378 nm. The SDS–PAGE protein analysis shows a single band corresponding to a molecular mass of ca 63 kDa (Fig. 1). The flavin coenzyme of the mSMO was non-covalently bound to the enzyme since it was released after treatment with hot methanol. Molar absorption coefficient of 11 $mM^{-1}cm^{-1}$ at 457 nm was calculated taking into account the molar absorption coefficient for FAD in methanol (11.3 $mM^{-1}cm^{-1}$), the molecular mass of mSMO, and the absorbance values of the native oxidized and methanol extracted enzyme.

The most canonical polyamines (Spm, Spd, Put) and their acetyl-derivatives were tested as substrates of mSMO. The unique substrate was Spm, indicating that the murine mSMO is preferentially active on this substrate and confirming previous results [13–15], but in contrast with data recently reported by Wang et al. [14] for the recombinant human PAOh1/SMO, which is capable of oxidizing also the N^1-AcSpm. Values of K_m, V_{max}, and pH optimum were determined using Spm as substrate. The calculated values (K_m = 170 μM, k_{cat} = 4.8 s^{-1}, and pH optimum 8.5) are in good agreement with the ones previously reported for this enzyme [15]. On the contrary, the values calculated for the human PAOh1/SMO enzyme [14] are different, the K_m being 1.63 μM and the V_{max} 7.72 μmol/mg protein/min (corresponding to a k_{cat} = 7.2 s^{-1}) at pH 9.0.

The MDL72,527 is a specific inhibitor of PAO activities [22,23]. This inhibitor has been largely used as a polyamine analogue and reversibly binds to the active site of the enzyme; on longer incubation times, it reacts with as yet unidentified chemical residues in the active site and inhibition becomes irreversible. As a consequence, two types of inhibition may be detected for MDL72,527, competitive and irreversible, depending on the incubation time. In living cells, as well as in experimental animals, MDL72,527 at micromolar concentration specifically inactivates PAOs time-dependently, without inhibiting other enzymes of polyamine metabolism (for a review see Seiler et al. [24]). Since mSMO is the last enzyme of the polyamine interconversion

Table 1
Summary of the procedure employed to purify mSMO

Purification step	Total vol. (ml)	Total activity (U)	Total protein (mg)	Specific activity (U/mg)	Purification	Yield
Crude extract	180	292	946	0.31	1	100
Hi Trap Q chromatography	116	180	160	1.12	3.6	62
Hi Trap butyl chromatography	52	96	42.8	2.24	7.2	33
Superdex 20HR chromatography	12	60	12	5.00	16.1	21

The enzyme activity and protein content of each sample were determined as described in the Experimental section. The specific activity of the extract is given in international units per milligram of total protein, and after the last step of the purification procedure corresponds, within the experimental error, to the activity of the pure enzyme as calculated from the k_{cat} values reported in Table 3. Purification is calculated as the increase of specific activity, and yield as the percentage of the total activity with respect to the value found in the crude extract.

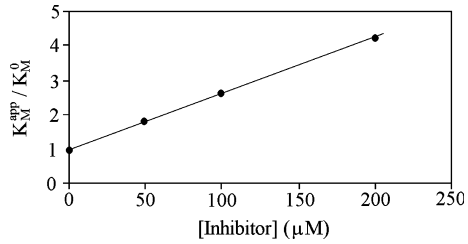

Fig. 2. Effect of MDL72,527 concentration on the K_m^{app}/K_m^0 ratio for the competitive inhibition of mSMO catalyzed oxidation of Spm. The continuous line was calculated according to the Eq. (1) with the K_i value of 63 μM. All data were obtained at pH 8.5 (0.2 M NaPi buffer).

pathway that awaits the detailed elucidation of its interactions with the MDL72,527 inhibitor, we carried out inhibition assay experiments.

As shown in Fig. 2, MDL72,527 competitively inhibited Spm oxidation catalyzed by mSMO. The affinity of MDL72,527 for mSMO was 63 μM. The incubation of the inhibitor with the purified mSMO resulted in a time dependent irreversible loss of enzyme activity; the half-time ($t^{1/2}$) of the reaction at 100 μM MDL72,527 was 15 min. The mechanism proposed in Scheme 1 implies that the apparent rate constant of irreversible inactivation is a function of the equilibrium dissociation constant K_I and the intrinsic half-time of the second reaction step (Eq. (2) in Experimental) and leads to an estimate of 9 min for the latter parameter. Exhaustive dialysis of the inactivated enzyme does not restore activity, and substrate addition to the irreversibly inhibited enzyme solution does not induce the MDL72,527 dissociation (i.e., the recovery of mSMO activity).

Two spectroscopically distinguishable intermediates can be identified during the catalytic cycle of this flavoenzyme, one oxidized, the other reduced. The steady state mixture can be accurately represented as a linear combination of the two (Fig. 3). Several kinetic schemes were tested and, although three steps schemes were able to describe each single time course, they showed significant systematic deviations when applied to the global analysis of the experiments reported in Fig. 4. The simplest kinetic mechanism capable of an acceptable description of the whole set of experimental data is reported in Scheme 1. The results of this analysis are shown in Fig. 4 where the model was used to fit a complex set of time courses collected at 460 nm, a wavelength where the oxidized flavine cofactor has a characteristic absorbance peak. Since for technical reasons more experiments were conducted starting from the oxidized than from the reduced enzyme, the minimization routine tended to overweight the former experiments at the expense of the latter. To correct this bias the variance of the pertinent time course was assigned twice the weight assigned to all other time courses; the rate constants obtained from this procedure are reported in Table 2.

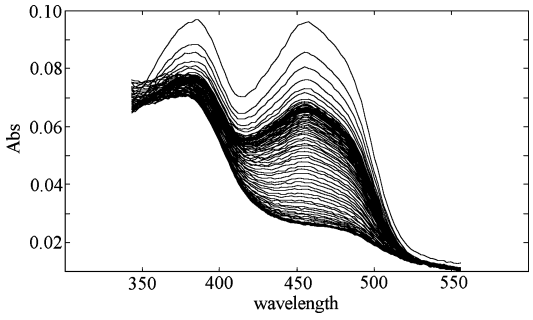

Fig. 3. Spectra recorded during the oxidation of Spm by mSMO. Experimental conditions as in trace 3 from Fig. 4.

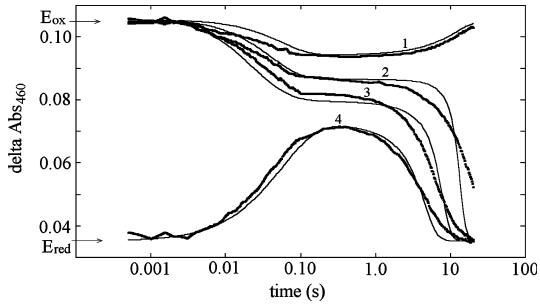

Fig. 4. Time courses of the oxidation of spermine by mSMO as followed at 460 nm. Experimental conditions: 0.2 M NaPi buffer, pH 8.5, $T = 25\,^{\circ}C$, 13 μM mSMO; substrate concentrations: trace 1, 160 μM Spm, 270 μM O_2; trace 2: 400 μM Spm, 270 μM O_2; trace 3: 1 mM Spm, 270 μM O_2; and trace 4: 1 mM Spm, 135 μM O_2 (all concentrations after mixing). Traces 1 through 3 were recorded after mixing oxidized mSMO with Spm (both solutions containing oxygen); trace 4 was recorded after mixing substrate reduced mSMO with oxygen containing buffer.

Although the disappearance of the substrates and the formation of the products are not measured directly in this type of experiment, the values of the rate constants determine unequivocally the steady state parameters (see Experimental). These are reported in Table 3, together with those directly determined. The agreement between the calculated and measured values is not as strict as we desired, but is acceptable, and suggests that Scheme 1, although simplified, provides a reasonable approximation of the catalytic cycle.

The analysis presented so far does not provide a good description of the events occurring at the very end of the time courses presented in Fig. 4. This is most probably due to an intrinsic property of the enzyme, rather than to artifacts or baseline shifts, and was consistently reproduced in our experiments. The easiest explanation of the discrepancy between the fit according to Scheme 1 and the experimental data is product inhibition, either reversible (by the aldehyde product) or irreversible (by hydrogen peroxide); this would progressively lower the activity of the enzyme as products accumulate, resulting in the slow exit from the steady state phase. Product

Table 2
Rate constants for the individual reactions of the catalytic cycle of mouse mSMO

k_1	k_{-1}	k_2	k_{-2}	k_3	k_4
$9.6\times10^4\,M^{-1}s^{-1}$	$10\,s^{-1}$	($46\,s^{-1}$)	($150\,s^{-1}$)	$28\,s^{-1}$	$7.8\times10^4\,M^{-1}s^{-1}$

k_1 and k_4 describe second order processes, whereas k_{-1}, k_2, k_{-2}, and k_3 correspond to first order ones. The values of k_2 and k_{-2} are undetermined (hence they are reported in parentheses) since they are so much higher than all the others; however, their ratio is well determined, and the table reports the lowest estimates for these parameters. Higher values of k_2 and k_{-2} with the same ratio would describe the experimental data equally well; the standard deviation of all other parameters is ≈30% of their value.

Table 3
Values of the steady state parameters for mSMO acting on Spm, as compared with the ones obtained from the individual rate constants reported in Table 2 (in parentheses)

k_{cat} $S_{O_2\,=\,270\,\mu M}$	K_m $S_{O_2\,=\,270\,\mu M}$	k_{cat} O_2 $_{S\,=\,1\,mM}$	K_m O_2 $_{S\,=\,1\,mM}$	k_{cat}
$4.8\,s^{-1}$	0.17 mM	—	—	—
($4.6\,s^{-1}$)	(0.12 mM)	($5.1\,s^{-1}$)	(63 μM)	($\leqslant 7\,s^{-1}$)

The values of k_{cat} and K_m for spermidine were determined as described in the Experimental section in air equilibrated samples. The values in parenthesis, for spermidine and for oxygen were calculated from the individual rate constants, as reported in Table 2. k_{cat} is the maximal activity of the enzyme, at infinite concentration of both substrates, and has a large uncertainty, due to the uncertainty in the determination of k_2 and k_{-2}.

inhibition is magnified in stopped flow experiments, due to the relatively high enzyme and substrate concentrations employed. Indeed, three out of the four time courses reported in Fig. 4 end up with the fully reduced enzyme (i.e., with low absorbance), due to exhaustion of the oxygen present in the reaction cell (either 270 or 135 μM). The hypothesis of product inhibition is further supported by the K_m for Spm calculated from the kinetic parameters being higher than that measured directly (Table 3).

Single turnover experiments yielded exponential time courses, whose dependence on the substrate concentration is compatible with an order lower than 2 (Fig. 5). This result is expected for any complex kinetic mechanism and simply demonstrates that the rate limiting step changes as a response to the concentration of the substrate, second order steps being rate limiting at low Spm concentration. The apparent pseudo first order rate constants of $3.6\,s^{-1}$ at 0.1 mM Spm and $6.5\,s^{-1}$ at 0.4–0.8 mM Spm are compatible with the known steady state parameters and suggest that the catalytic mechanism does not change as a response to wide variations in the relevant experimental conditions.

A more refined analysis was carried out by asking the minimization routine to consider at the same time single turnover and steady state experiments, in order to ensure that the set of parameters obtained is internally coherent: indeed, as it often occurs with complex kinetic schemes, minimization according to Scheme 1 may yield multiple minima. This analysis confirmed that the parameters reported in Table 2 are compatible with the single turnover experiments.

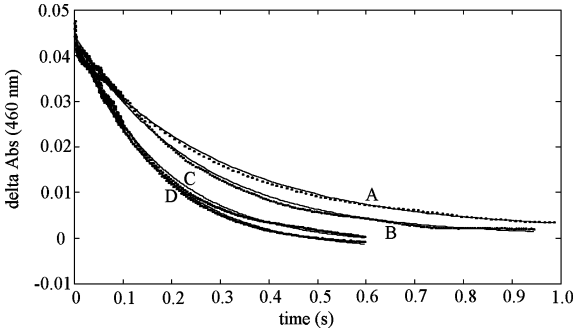

Fig. 5. Time courses of the reduction of mSMO by Spm in the absence of oxygen (single turnover experiments). Experimental conditions: mSMO concentration 14 μM throughout; all the experiments of this series were carried out in the absence of O_2; any possible contamination by the gas was removed by adding glucose (5 mM), glucose oxidase, and catalase; spermine concentration: trace A, 100 μM; trace B, Spm 200 μM; trace C, Spm 400 μM; and trace D, Spm 800 μM. All concentrations are after mixing; other conditions as in the multiple turnover experiments (Fig. 4).

Discussion

Purification and biochemical features of the recombinant mSMO

The mSMO recombinant enzyme was expressed at a level of about 20 U/L of culture broth. Further purification of the mature form of this enzyme has been achieved by three chromatographic steps (Table 1), obtaining a protein product virtually free of contaminants. Due to the high yield of purified mSMO enzyme after expression in *E. coli*, its substrate specificity has been definitively determined using different polyamines and acetyl-derivatives.

Spm is the only specific substrate for the murine recombinant enzyme, confirming previously data published by Vujcic et al. [11] and Cervelli et al. [15]. It is worth mentioning that recently Wang et al. [14] have

reported that the human recombinant PAOh1/SMO is able to oxidize N^1-AcSpm, albeit in less extent. Furthermore, the human enzyme shows a K_m value 100 times lower (K_m = 1.6 μM) [14] than the one found for mSMO ([15] and the present paper). We like to point out that concerning the K_m data of the human PAOh1/SMO enzyme, different values have been reported up to now [12,14]. On the contrary, the K_m and k_{cat} values obtained directly and calculated by rapid kinetic experiments in the present paper for the murine recombinant enzyme are congruent. The discrepancy observed in substrate specificity and kinetic parameters for the human and murine SMO enzymes remains to be elucidated.

Specific SMO inhibitors may represent important tools in studying the catalytic mechanism of SMO. They may also be valuable tools in unraveling the physiological role of this class of enzymes in animal cell growth and differentiation and in designing new antineoplastic drugs. With this in mind, we carried out inhibition assay experiments on the SMO enzymatic activity in the presence of the PAO inhibitor MDL72,527 [22–24]. We observed that MDL72,527 competitively inhibited Spm oxidation catalyzed by mSMO. However, the affinity of MDL72,527 for mSMO (i.e., 63 μM) was lower than that observed for the pig liver PAO (~0.1 μM) by Bey et al. [22] and Federico et al. [25]. Incubation of the inhibitor with the purified mSMO resulted in a time- and dose-dependent loss of enzyme activity. The mSMO half-life calculated for saturating concentration of MDL72,527 is lower than that reported by Bey et al. [22] for pig liver PAO ($t_{1/2}$ = 2.2 min). This is not inconsistent with the lower affinity of mSMO, that indicates reduced stability of the initial, reversible complex even though the value is extrapolated for saturating inhibitor concentration. The mSMO inhibition results presented in this paper and data reported by Bey et al. [22] for the pig liver PAO are congruent with the ones reported by Vujcic et al. [11], describing that the enzymatic activities of murine SMO and PAO from crude extract were inhibited when the inhibitor was added prior to the addition of the substrates Spm and N^1-AcSpm, respectively, and that the MDL72,527 inhibits less efficient mSMO than the PAO enzyme.

The analysis of rapid kinetic experiments reveals some interesting features of mSMO, namely the rapid second order oxidation reaction by dioxygen and the slow exhaustion of substrate which follows the steady state phase. The reoxidation of flavine-containing amine oxidases from plants is characteristically fast and second order and does not show evidence for the presence of the semiquinone intermediate observed in other flavoenzymes; this property has often be an used to classify these enzymes and is shared by mSMO. The exit of the enzyme from the steady state, associated to the exhaustion of oxygen, poorly fitted in the experiments presented in Fig. 4, may be explained by the inhibition by product; this is consistent with the observed difference between the values of K_m obtained directly and calculated from the kinetic parameters (see Tables 2 and 3). In this respect it is also worth noting the good agreement between the values of k_{cat}, again consistent with the hypothesis of product inhibition, since in this analysis k_{cat} is expected to be much less affected than K_m.

Because of the absolute requirement of polyamines for cell growth, mammalian polyamine metabolism has been demonstrated to be an important target of antitumor drug development. In fact, some of the most effective antineoplastic polyamine analogues, concerning symmetrically and asymmetrically substituted polyamines, are capable to dramatically modify the polyamine metabolism [5,7,26,27]. Recent studies focused on the role of mammalian SMO relied on the availability of specific clones [12,14,15]. The heterologous expression of the recombinant mSMO enzyme presented here provides a tool and offers some unique opportunity insights into the regulation and importance of SMO. Moreover, it will allow to test the specificity of many antitumor polyamine analogues, which can be further utilized in tumorigenic studies.

Acknowledgments

The authors are grateful to Ms. Roberto Da Gai, Servizio Biologico, Istituto Superiore di Sanità di Roma, for technical assistance. This research was supported by grants from "Ministero Istruzione, Università e Ricerca" (MIUR) and "Consiglio Nazionale Ricerca" (CNR) Target Project "Biotechnology."

References

[1] W.S. McIntire, C. Hartman, in: V.L. Davison (Ed.), Principle and Application of Quinoproteins, Marcel Dekker, New York, 1993, pp. 97–171.
[2] N. Seiler, Polyamine oxidase, properties and functions, Prog. Brain Res. 106 (1995) 333–344.
[3] R.J.M. Den Munckhof, M. Denyn, W. Tigchelaar-Gutter, R.G. Schipper, A.A.J. Verhofstad, C.J.F. Van Noorden, W.M. Frederiks, In situ substrate specificity and ultrastructural localization of polyamine oxidase activity in unfixed rat tissues, J. Histochem. Cytochem. 43 (1995) 1155–1162.
[4] A.E. Pegg, R.H. Hu, Effect of polyamine analogues and inhibition of polyamine oxidase on spermidine/spermine N1-acetyltransferase activity and cell proliferation, Cancer Lett. 95 (1995) 247–252.
[5] R.J. Bergeron, Y. Feng, W.R. Weimar, J.S. McManis, H. Dimova, C. Porter, B. Raisler, O.A. Phanstiel, A comparison of structure–activity relationships between spermidine and spermine analogue antineoplastics, J. Med. Chem. 40 (1997) 1475–1494.
[6] H.C. Ha, P.M. Woster, J.D. Yager, R.A. Casero Jr., The role of polyamine catabolism in polyamine analogue-induced programmed cell death, Proc. Natl. Acad. Sci. USA 94 (1997) 11557–11562.

[7] R.A. Casero Jr., P.M. Woster, Terminally alkylated polyamine analogues as chemotherapeutic agents, J. Med. Chem. 44 (2001) 1–26.
[8] E. Hölttä, Oxidation of spermidine and spermine in rat liver: purification and properties of polyamine oxidase, Biochemistry 16 (1977) 91–100.
[9] P.R. Libby, C.W Porter, Separation of two isozymes of polyamine oxidase from murine L1210 leukemia cells, Biochem. Biophys. Res. Commun. 144 (1987) 528–535.
[10] T. Tsukada, S. Furusako, S. Maekawa, H. Hibasami, K. Nakashima, Purification by affinity chromatography and characterization of porcine liver cytoplasmic polyamine oxidase, Int. J. Biochem. 20 (1988) 695–702.
[11] S. Vujcic, P. Liang, P. Diegelman, D.L. Kramer, C.W. Porter, Genomic identification and biochemical characterization of the mammalian polyamine oxidase involved in polyamine back-conversion, Biochem. J. 370 (2003) 19–28.
[12] Y. Wang, W. Devereux, P.M. Woster, T.M. Stewart, A. Hacker, R.A. Casero Jr., Cloning and characterization of a human polyamine oxidase that is inducible by polyamine analogue exposure, Cancer Res. 61 (2001) 5370–5373.
[13] S. Vujcic, P. Diegelman, C.J. Bacchi, D.L. Kramer, C.W. Porter, Identification and characterization of a novel flavin-containing spermine oxidase of mammalian cell origin, Biochem. J. 367 (2002) 665–675.
[14] Y. Wang, T. Murray-Stewart, W. Devereux, A. Hacker, B. Frydman, P.M. Woster, R.A. Casero Jr., Properties of purified recombinant human polyamine oxidase, PAOh1/SMO, Biochem. Biophys. Res. Commun. 304 (2003) 605–611.
[15] M. Cervelli, F. Polticelli, F. Rodolfo, P. Mariottini, Heterologous expression and characterization of mouse spermine oxidase, J. Biol. Chem. 278 (2003) 5271–5276.
[16] M. Cervelli, A. Bellini, M. Bianchi, L. Marcocci, S. Nocera, F. Polticelli, R. Federico, R. Amendola, P. Mariottini, Mouse spermine oxidase gene splice variants: nuclear sub-cellular localization of a novel active isoform, Eur. J. Biochem. 271 (2004) 760–770.
[17] J. Sambrook, E.F. Fritsch, T. Maniatis, Molecular Cloning: A Laboratory Manual, second ed., Cold Spring Harbor Laboratory, Cold Spring Harbor, NY, 1989.
[18] T.A. Smith, J.H. Barker, The di- and polyamine oxidase of plants, in: V. Zappia, A.E. Pegg (Eds.), Progress in Polyamine Research: Novel Biochemical, Pharmacological and Clinical Aspects, Plenum Press, New York, 1988, pp. 573–589.
[19] M.M. Bradford, A rapid and sensitive method for the quantitation of microgram quantities of protein utilising the principle of protein-dye binding, Anal. Biochem. 72 (1976) 248–254.
[20] U.K. Laemmli, Cleavage of structural proteins during assembly of the head of bacteriophage T4, Nature 277 (1970) 680–685.
[21] A. Bellelli, L. Morpurgo, B. Mondovì, E. Agostinelli, The oxidation and reduction reactions of bovine serum amine oxidase. A kinetic study, Eur. J. Biochem. 267 (2000) 3264–3269.
[22] P. Bey, F.N. Bolkenius, N. Seiler, P. Casara, *N*-2,3-Butadienyl-1,4-butanediamine derivatives: potent irreversible inactivators of mammalian polyamine oxidase, J. Med. Chem. 28 (1985) 1–2.
[23] F.N. Bolkenius, P. Bey, N. Seiler, Specific inhibition of polyamine oxidase invivo is a method for the elucidation of its physiological role, Biochim. Biophys. Acta 838 (1985) 69–76.
[24] N. Seiler, B. Duranton, F. Raul, The polyamine oxidase inactivator MDL72527, Prog. Drug Res. 59 (2002) 1–40.
[25] R. Federico, L. Leone, M. Botta, C. Binda, R. Angelini, G. Venturini, P. Ascenzi, Inhibition of pig liver and Zea mays L. polyamine oxidase: a comparative study, J. Enzyme Inhib. 16 (2001) 147–155.
[26] R.A. Casero Jr., P. Celano, S.J. Ervin, C.W. Porter, R.J. Bergeron, P.R. Libby, Differential induction of spermidine/spermine N^1-acetyltransferase in human lung cancer cells by the bis(ethyl)polyamine analogues, Cancer Res. 49 (1989) 3829–3833.
[27] L. Alhonen, A. Karppinen, M. Uusi-Oukari, S. Vujcic, V.P. Korhonen, M. Halmekyto, D.L. Kramer, R. Hines, J. Jänne, C.W. Porter, Correlation of polyamine and growth response to N^1,N^{11}-diethylnorspermine in primary fetal fibroblasts derived from transgenic mice overexpressing spermidine/spermine M1-acetyltransferase, J. Biol. Chem. 273 (1998) 1964–1969.